Eur. Phys. J. B (2012)
DOI: 10.1140/epjb/e2012-30413-7

THE EUROPEAN PHYSICAL JOURNAL B

Regular Article

Structural evolution of the tropical pacific climate network

L.C. Carpi[1], P.M. Saco[1,a], O.A. Rosso[2,3,4], and M.G. Ravetti[5]

[1] Civil, Surveying and Environmental Engineering. The University of Newcastle, University Drive, 2308 Callaghan NSW, Australia
[2] LaCCAN/CPMAT – Instituto de Computação, Universidade Federal de Alagoas BR 104 Norte km 97 57072-970 Maceió, Alagoas, Brazil
[3] Laboratorio de Sistemas Complejos, Facultad de Ingeniería. Universidad de Buenos Aires, 1063 Av. Paseo Colón 840, Ciudad Autónoma de Buenos Aires, Argentina
[4] Fellow CONICET, Argentina
[5] Departamento de Engenharia de Produção, Universidade Federal de Minas Gerais, Av. Antônio Carlos, 6627, Belo Horizonte, 31270-901 Belo Horizonte – MG, Brazil

Received 23 May 2012 / Received in final form 8 September 2012
Published online (Inserted Later) –

Abstract. A new methodology based on information theory is used to explore the evolution of the surface air temperature climate network over the Tropical Pacific region. Topological changes over the period 1948–2009 are investigated using windows of one year duration. Alternating states of lower/higher efficiency in information transfer are consistently captured during the opposing phases of ENSO (i.e., El Niño and La Niña years). This cyclic information transfer's behavior reflects a higher climatic stability for La Niña years which is in good agreement with current observations. In addition, after the 1976/77 climate shift, a change towards more frequent conditions of decreased information transfer efficiency is detected.

1 Introduction

El Niño/Southern Oscillation (ENSO), an occasional and quasiperiodic shift in winds and ocean currents centered in the Tropical Pacific region, is linked to anomalous global climate patterns responsible for producing world-wide socioeconomi c impacts. La Niña effects on global weather variability are approximately opposite to those of El Niño [1], and the atmospheric response to strong La Niña events tends to be weaker than that of the strong El Niño events [2]. In this work, we investigate the changes in the structure of the Tropical Pacific climate network using a novel approach based on complex network theory in order to gain new insights into the dynamical changes associated to the El Niño/Southern Oscillation.

During the last decade, the development and use of complex networks theory has led to major advances in the analysis of the behavior of dynamical systems in numerous areas of science [3] and references therein. Applications of complex networks to climate are recent and based on the premise that climate dynamics can be represented as a network of interacting units, with information (matter and energy) flowing between them [4,5]. When this information, carried by the flow of matter and energy, is transferred between these units (nodes), a link is created. In practice, the climate network is constructed using a global climate dataset. Each grid point in the spatial grid represents a node and links are created for pair of nodes that show significant statistically interdependence (for example, significant correlation). Excellent introductory descriptions of the theory and construction of climate networks can be found in the review papers [6,7].

The analysis of climate networks has provided valuable insights into different aspects of the climate dynamics that could not be captured using the classic methods frequently used in climatology like principal component or singular spectrum analysis [4–15]. These novel insights include the identification of super-nodes related to teleconnection patterns of the atmosphere [6], the presence of "small-world" properties due to long range connections in the climate network [6], and wave-like structures of high energy flow related to global surface ocean currents [7]. Additional work on climate networks [4] comparing results from two climate networks, one constructed from the global surface temperature data for all El Niño years and the other with the data for all La Niña years, showed that the number of total network links decreases for El Niño years and that this change is related to a decrease in information transfer and thus on predictability of climatic variables. Further understanding on network structural changes between El Niño and non-El-Niño time periods over various geographic regions has been recently obtained by analyzing the temporal evolution of the number of network links [5,12], and the presence of unstable or blinking links during El Niño [16].

Here we use a novel integrative approach that enables us to further investigate the temporal evolution of the

[a] e-mail: patricia.saco@newcastle.edu.au

climate network for the Tropical Pacific region. We track structural changes related to ENSO dynamics, and we are able to identify changes for individual El Niño and La Niña events, by computing the network topology for sliding temporal windows of one year duration over a record of 62 years. Local and global network properties are analyzed by quantifying the number of links, efficiency, average clustering coefficient and average path length. A new quantifier based on Information Theory recently developed for the analysis of dynamic network evolution [17] is used to compute changes in topological randomness. We also investigate changes in the connectivity pattern which helps us identify spatial differences in network characteristics for individual ENSO events. Unlike previous work, this approach allows us to analyze not only the general structural/topological differences between El Niño and La Niña networks for individual events, but also to isolate more subtle spatial network differences among them (for example, for the El Niño events of 1997 and 2002 that had unusual impacts on Australian rainfall [18]).

2 Methodology

The climate network was constructed using monthly averaged surface air temperature (SAT) data over the Tropical Pacific region ($120E°$–$70W°$, $20N°$–$20S°$) for the period 1948–2009. This type of network structure (ie., constructed using SAT data) has also been used in previous studies to enable capturing the dynamics of the heat exchange at the interface between ocean and atmosphere [10,19]. The dataset used corresponds to the reanalysis data distributed by the National Center for Environmental Prediction/National Center for Atmospheric Research (NCEP/NCAR), which is organized on a grid with resolution of 2.5×2.5 (lat-lon) [20]. Consequently, the resulting grid for the Tropical Pacific region has a total of 1156 nodes (17×68 nodes). The evolution of the network topology, from 1948 to 2009, was followed by considering 62 annual non-overlapping windows corresponding to the January to December monthly values. The network topology for each window was constructed by computing the Spearman's rank correlation coefficient, at lag zero, between the SAT time series of all possible pairs of nodes. Links were created for pairs of nodes with an absolute value of correlation over a prescribed threshold. We analyzed network structures obtained from the SAT time series, as well as those obtained from the anomaly SAT series in which seasonality was removed using standard procedures.

The identification of suitable thresholds is important as it can potentially change the network topology [7,21]. The selection of this appropriate threshold depends not only on the network characteristics (i.e, data used to generate the network) but also on the size of the network considered. For this particular case, the region considered is small and highly connected. We therefore conducted a sensitivity analysis to determine the impact of choosing different threshold values in a wide range from 0.6 to 0.9. Table 1 shows the increase in the average number of edges for the networks generated with decreasing threshold values. We found that the dynamics of the network (as identified by the various quantifiers described below) does not change significantly for values between 0.9 to 0.7. However the higher threshold value, 0.9, was best at identifying minor temporal changes in network topology and differences between El Niño and La Niña events and was therefore selected for the analysis described below.

Table 1. Average number of edges for varying values of threshold. The third column corresponds to the ratio of the average number of edges to the number of edges of a complete graph with the same number of nodes.

Threshold Value	Average number of edges	Average edges/Edges complete graph
0.9	68811.91	0.1031
0.8	166579.73	0.2495
0.7	253433.35	0.3796
0.6	332850.40	0.4986

Changes in the annual network topologies were analyzed by computing the standard quantifiers currently used in complex network analysis, that is, clustering coefficient, average path length, and network efficiency. The clustering coefficient indicates the number of links over all possible connections between neighbours of a given node. The average network clustering coefficient was computed for each annual network. The clustering coefficient obtained for a real network is usually compared to that of regular networks (characterized by the having same number of links for all nodes). Another useful quantifier used here is the average path length, which is calculated as the shortest distance (minimum number of links) between two nodes, averaged over all pairs of linked nodes in the network.

Network properties were also analyzed using the concept of efficient informational exchange through the network. By assuming that information transfer is easier between nodes connected by short paths, efficiency is defined as the inverse of the characteristic path length [22]. This quantifier was normalized by dividing by the maximum possible value, which is the efficiency corresponding to a fully connected graph. Unlike average path length that has an undetermined (infinite) value for disconnected nodes, the efficiency can be determined and has a value of zero in those nodes.

Finally, we also used a new quantifier, the square root of the Jensen Shannon divergence ($\mathcal{J}^{1/2}$) that, unlike the standard quantifiers currently used for network analysis, is independent of the number of links in the network [17]. It therefore allows for an improved comparison of network topologies with varying number of links, as the ones considered here. Another advantage of the $\mathcal{J}^{1/2}$ quantifier is that it is a metric that satisfies the triangle inequality [23,24]. It can be therefore used to compare various network topologies by measuring differences among the probability distribution functions (PDFs) of nodes links, also called node degree distribution. $\mathcal{J}$ is defined as,

$$\mathcal{J}[P, P_{ref}] = S[(P + P_{ref})/2] - S[P]/2 - S[P_{ref}]/2 \quad (1)$$

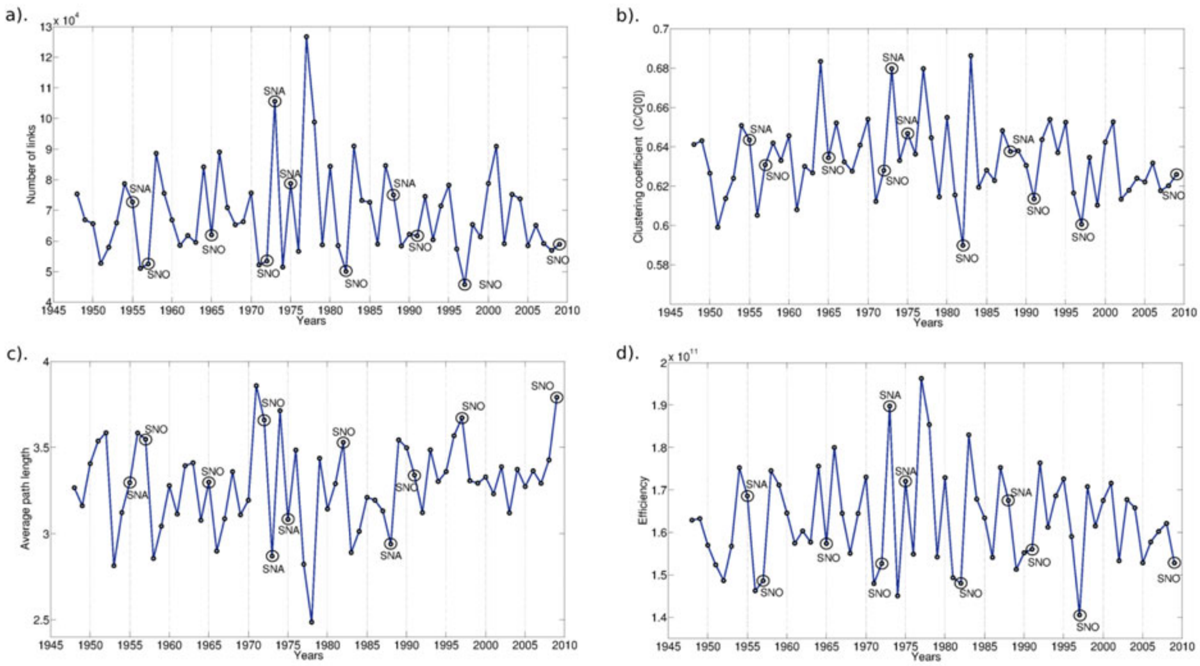

Fig. 1. (Color online) Evolution of network topology as captured by: (a) number of links, (b) average normalized clustering coefficient, (c) average path lenght, and (d) efficiency. Strong recorded ENSO events are indicated as SNO for El Niño and SNA for La Niña.

where P is the PDF of the node degree distribution, P_{ref} corresponds to a reference PDF, and S is the Shannon entropy, calculated as $S = -\sum p_i \log(p_i)$. Here we use the uniform distributionas P_{ref}, which corresponds to the asymptotic case of a random network topology structure, for which all nodes would have a random number of links. Therefore $\mathcal{J}^{1/2}$ provided, for each of the 62 windows, a measure of dissimilarity (or distance) to the asymptotic random structure. Higher values indicate that the topology is more distant to the reference structure and closer to a regular structure in which all nodes have the same number of links. A more detailed description of of this quantifier is available in reference [17], which includes an example of its application to a simpler network structure.

3 Results

3.1 Complex network evolution analysis

We investigated the temporal evolution of the network topology, and found that the ENSO signature was more clearly captured in the results obtained from the analysis of the original SAT data than in those obtained from SAT anomalies. We therefore present below the results from the networks obtained for the original SAT data.

Figure 1 shows the temporal evolution of the climate network topology as captured by the standard complex network quantifiers: number of links (a), average clustering coefficient (b), average path length (c), and efficiency (d). This figure also shows years corresponding to strong El Niño and La Niña events, identified using the Oceanic Niño Index (ONI). ONI is the standard index that NOAA uses for identifying El Niño (warm) and La Niña (cool) events in the tropical Pacific. It is obtained from the three-month running mean of the reconstructed sea surface temperature (SST) anomalies in the Niño 3.4 region [25]. Values of ONI are available through the National Oceanic and Atmospheric Administration (NOAA) climate prediction center (`http://www.cpc.noaa.gov`).

As seen from Figure 1, throughout the study period the dynamic climate network has large average clustering coefficient and small average path length values; these network properties are consistent with those of small world networks frequently found in real-world systems [7]. This figure also shows that temporal variations in all these measures reflect a cyclic behavior consistent with that of ENSO. There is a clear tendency for networks obtained for all the strong La Niña years to display lower average clustering coefficients, higher average path lengths and lower number of links than the networks corresponding to strong El Niño years. As expected for networks with fewer links and higher average path length, the efficiency for El Niño years is lower than that of La Niña years (Fig. 1d).

Figure 2 shows the temporal variability of $\mathcal{J}^{1/2}$, also consistent with the ENSO cyclic behavior. In this figure, we also include years corresponding to both strong and moderate El Niño and La Niña events identified using ONI. As mentioned before, the metric properties of the $\mathcal{J}^{1/2}$ quantifier and its independence from the total number of links makes it particularly suitable for comparing the characteristics of the evolving network topology analyzed in this study, where the number of links changes with time. Though the degree distribution

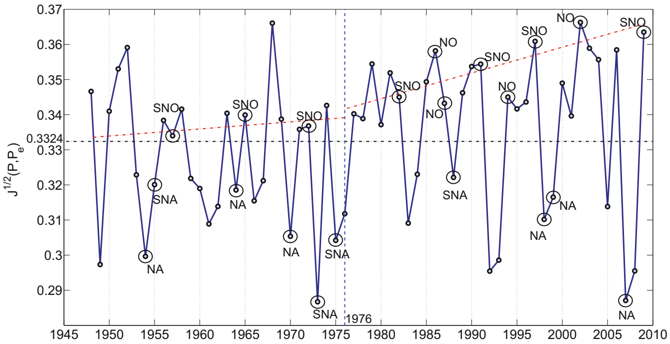

Fig. 2. (Color online) Evolution of the square root of the Jensen-Shannon divergence, $\mathcal{J}^{1/2}(P, P_e)$, for the Tropical Pacific region. Strong and moderate ENSO events are indicated as SNO and NO for El Niño and SNA and NA for La Niña respectively. The vertical dashed line indicates the 76/77 climate shift and the red lines show trends in $\mathcal{J}^{1/2}(P, P_e)$ computed for all El Niño events before and after the shift.

maintains approximately the same distance to the reference uniform distribution P_e throughout the study period, the $\mathcal{J}^{1/2}$ values corresponding to all moderate and strong La Niña and El Niño years are respectively below and above the average value of $\mathcal{J}^{1/2}$ (horizontal dashed line). This means that the structure for El Niño years is closer to that of regular networks, and therefore less efficient in transferring information. These results are consistent with previous findings by Tsonis and Swanson [19] that show that the number of links decreases for El Niño events, and as a result both the flow of information and predictability decrease.

It is important to note that the efficiency of the climate network can be interpreted in terms of the potential effects of local fluctuations, which tend to have a destabilizing effect in its source region. These fluctuations, which are equivalent to information in network analysis, are transferred through the network. If this transfer is efficient then the possibility of prolonged local fluctuations (as for example local extremes) is reduced, providing more stability to the system [4]. Consequently, more regular structures, as those corresponding to El Niño years, could be associated to strong local events that are not efficiently transferred or dampened by the network structure.

Another interesting observation, evident from the dynamical analysis of the network structure and captured by the evolution of $\mathcal{J}^{1/2}$ displayed in Figure 2, is a change in dynamics occurring approximately after the 1976/1977 time period. This change in the dynamics of the network structure coincides with the 76/77 climate shift extensively discussed in the literature [26,27]. As noted in the literature, the intensity and frequency of El Niño events increased after the climate shift. Our analysis detects that this climate shift gives rise, on average, to a more regular climate network as shown by the more frequent values of $\mathcal{J}^{1/2}$ above the horizontal line after 76/77. The red lines in Figure 2 show the linear trends fitted to the values of $\mathcal{J}^{1/2}$ for El Niño events before and after 1976. These trends highlight that peak values of $\mathcal{J}^{1/2}$ for El Niño events are not only more frequent but also higher for the post-shift period. Therefore, the network after the climate shift exhibits conditions of less efficient information transfer that could be associated to a less stable climate with more frequent and intense local extreme events.

3.2 Evolution of the network connectivity pattern

The dynamic evolution of the network structure was also investigated by inspecting the temporal changes in the network connectivity pattern. In large dynamic networks, the most connected nodes (nodes with higher degree or number of links) tend to change over time [28]. We found that temporal changes in the most connected nodes for the Tropical Pacific climate network are consistent with the cyclic nature of ENSO. As seen from Figures 3 and 4, we found a consistent connectivity pattern for all the strong El Niño events, which is clearly distinct from the also consistent pattern found for the strong La Niña years. While both networks connectivity patterns display similar highly connected regions in the upper portion of the window, the features in the central and lower portions are distinctly different. It can be observed that in all strong La Niña events there is a large region with high connectivity that extends from the South American Peruvian coast spreading over the whole lower southeastern quadrant of the window and beyond. This large area of high connectivity is not present for the strong El Niño events, which instead show a smaller area with high connectivity close to the Northeastern Australian coast that extends to the east, and is mostly located south of the $10S^{\circ}$ latitudinal circle. Figures 3 and 4 corroborate our previous discussion on network efficiency by showing that highly connected areas for El Niño are smaller in size than those for La Niña networks, and therefore a higher capacity for information transfer in La Niña events.

We also found that the connectivity patterns for all moderate El Niño (1986, 1987, 1994, and 2002) and La Niña (1954, 1964, 1970, 1998, 1999, and 2007) events are very similar to those of the strong events shown in Figures 3 and 4, that is, a smaller area with high connectivity close to the Northeastern Australian coast that extends to the east for El Niño years, and the larger connectivity area extending over the entire lower SE quadrant for La Niña. As an example of El Niño, Figure 5 displays the connectivity pattern for the moderate 2002 event which, in addition, has one of the highest $\mathcal{J}^{1/2}$ values. This event has been extensively analyzed in the literature because it produced extremely severe drought conditions in Australia, usually associated to the stronger events. Moreover, the conditions for this event are frequently compared to those of the 1997 event, which had an unusually weak impact in Australia despite being the strongest EL Niño on record according to various ENSO indices [18]. Hackert et al. [29] compare the development of both events by considering their initial conditions and the atmospheric forcing. They found that initial conditions played a larger role on the 2002 event than in the 1997 event, in which forcings played a more dominant role. In terms of network connectivity structure,

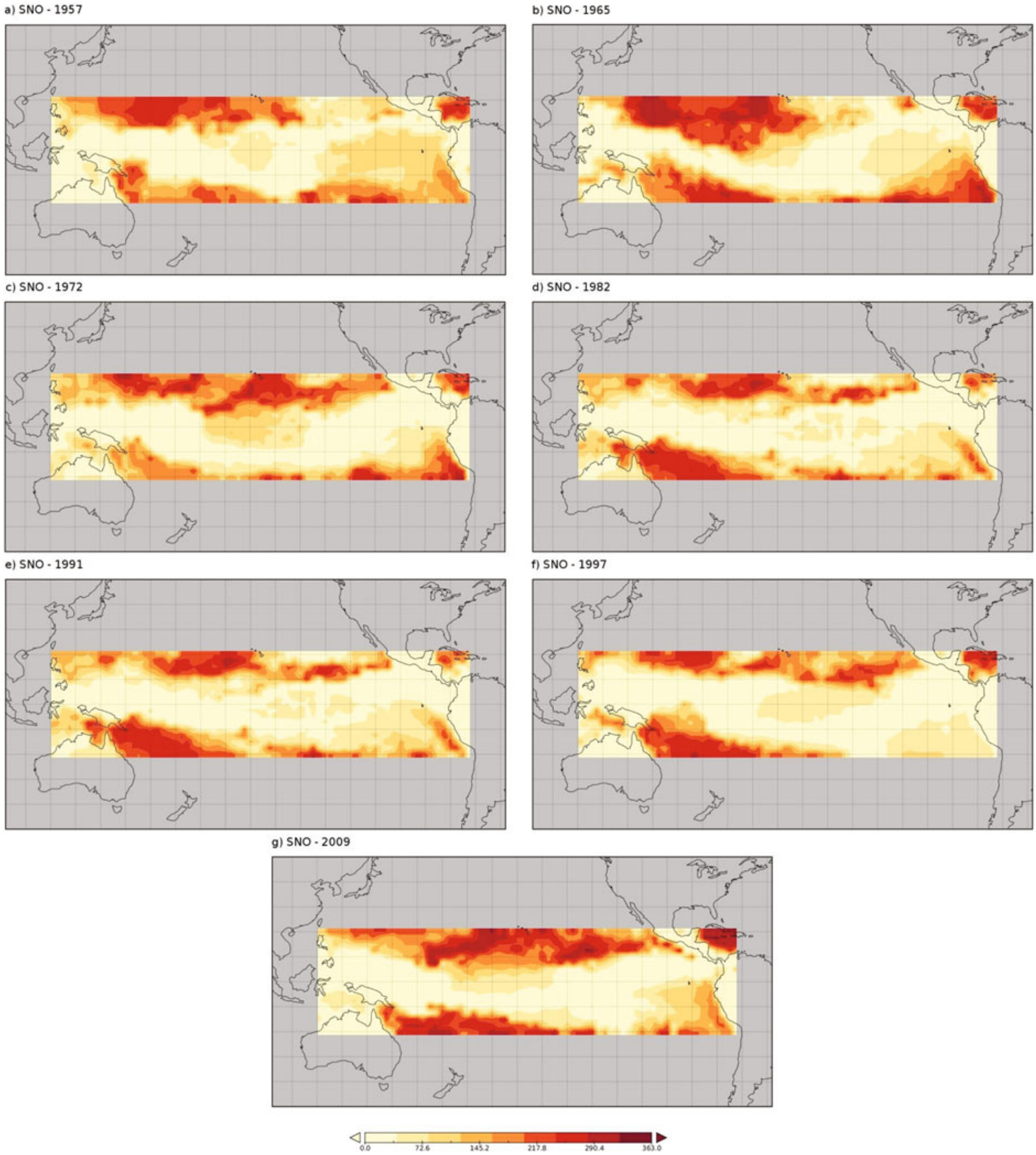

Fig. 3. (Color online) Connectivity patterns corresponding to strong El Niño years: (a) 1957, (b) 1965, (c) 1972, (d) 1982, (e) 1991, (f) 1997, (g) 2009.

we find that the 2002 event shows more similarity to all the other strong events than the pattern for the 1997 event. This last one displays lower connectivity in the Peruvian South American coast.

Finally we examined the SAT network characteristics for the weak ENSO events. We found that, similarly to the strong and moderate events, most weak El Niño years (1951, 1963, 1968, 1969, 1977, 2004, 2006) display values of $\mathcal{J}^{1/2}$ (Fig. 2) above average, with the only exception of the 1976 event whose value is below average. Though for half of the years the spatial patterns are very similar to those of the strong and moderate el Niño years, the others (1969, 1976, 1977, 2004) show some small departures mainly in the form of larger clusters of high connectivity. One of these events, that shares remarkable similarity in network connectivity to the strong events and displays a very high $\mathcal{J}^{1/2}$ value is the 2006 event (Fig. 6). In fact, this particular El Niño was studied by McPhaden [30] who reported a detailed analysis of the climate conditions for this event, concluding that it had an unusual development that was weakened by external influences. Furthermore, he suggested that the co-occurrence of El Niño and the Indian

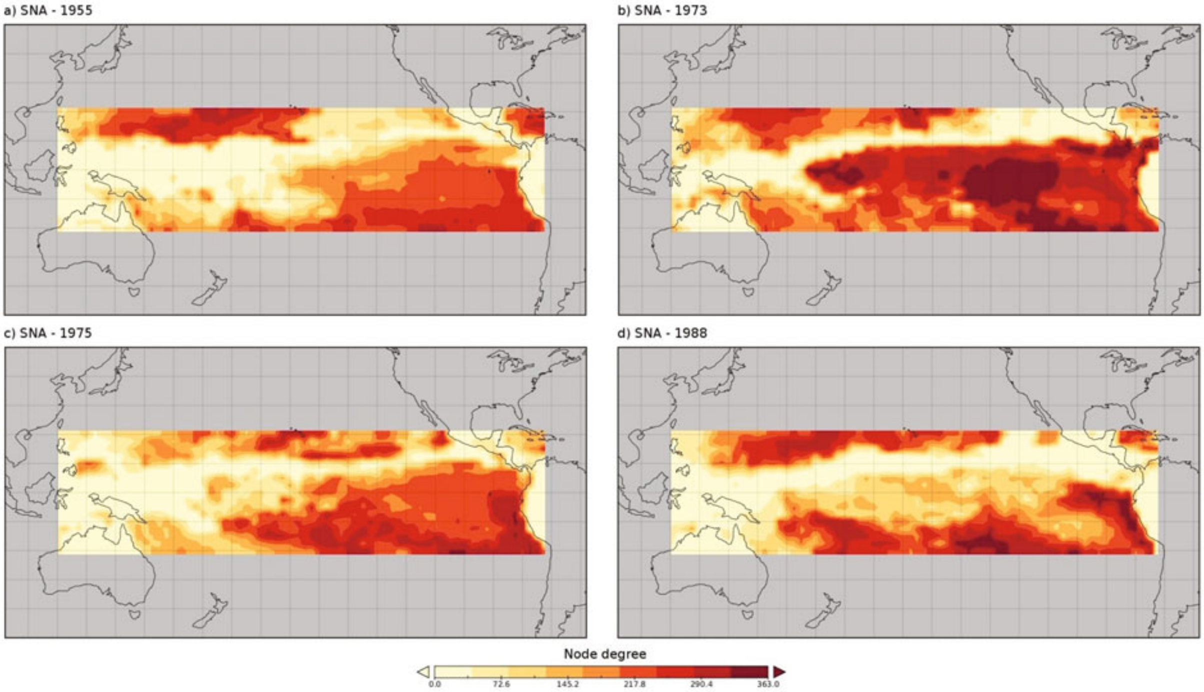

Fig. 4. (Color online) Connectivity patterns corresponding to strong La Niña years: (a) 1965, (b) 1973, (c) 1975, (d) 1986.

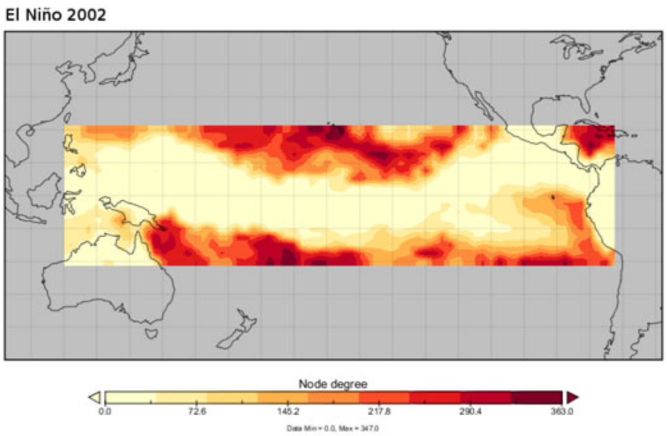

Fig. 5. (Color online) Connectivity pattern for the 2002 El Niño event.

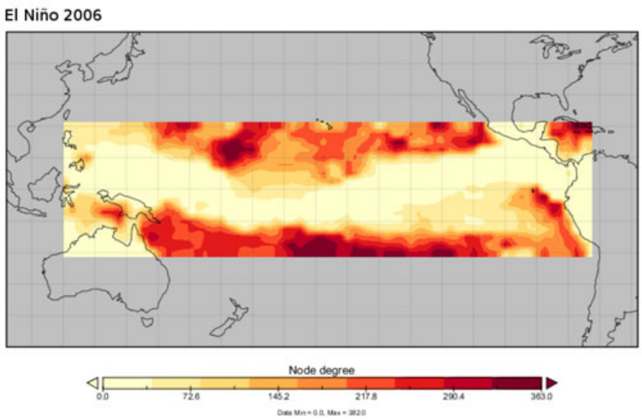

Fig. 6. (Color online) Connectivity pattern for the 2006 El Niño event.

Ocean dipole/zonal mode events created conditions for the demise of this El Niño. Nevertheless, this event still had strong impacts in several regions of the world, like drought in Australia and Indonesia, and a reduction in the intensity and number of hurricanes in the Atlantic.

The weak La Niña events do not show the same consistency. The network characteristics depart from those of the moderate and strong La Niña years as shown by $\mathcal{J}^{1/2}$ (Fig. 2). Unlike the strong and moderate events, the value of $\mathcal{J}^{1/2}$ for the weak 1950, 1956, 1971, 1974, 1995, and 2000 events is above average. Only the 1962, 1967,and 1984 events, have a value of $\mathcal{J}^{1/2}$ below average. The patterns in this case tend to depart from those of the strong La Niña years, with smaller high correlations clusters in the lower SE quadrant (particularly for the events with higher $\mathcal{J}^{1/2}$ values).

4 Conclusions

We presented a novel and integrative approach that enabled us to investigate the temporal evolution of the SAT climate network for the Tropical Pacific region by computing the dynamic network topology for temporal windows of one year duration over the 1948–2009 record. This methodology enables the analysis of dynamic networks and therefore can be useful for other climate applications.

Using this approach, we found that the dynamic network topology clearly displays a cyclic behavior consistent with that of ENSO, with topologies for the strong and moderate El Niño networks closer to a regular network structure and therefore less efficient than those of the strong and moderate La Niña events. The existence of larger highly connected areas on the patterns of La Niña networks also demonstrates their higher information transfer efficiency.

This behaviour is consistent with the observation reported by McPhaden [2] who pointed out that the strong La Niña events tend to have a weaker atmospheric response than that of the strong El Niño events. This difference is attributed to the fact that the decrease in tropical rainfall induced by colder conditions on the tropical Pacific Ocean temperatures (which produces atmospheric heating and the associated teleconnection patterns) is constrained by a lower limit of zero. This constraint could be responsible for the increase in highly correlated nodes for La Niña events that gives rise to the larger highly connected areas in the La Niña patterns. However as also pointed out in reference [2], the rainfall increase for the strong El Niño events is not subjected to an upper constraint and therefore neither is the resulting atmospheric heating.

Though the previous results for the strong and moderate El Niño years are also generally valid for the weak El Niño networks, the results for the weak La Niña networks are not as consistent. Most of the weak La Niña events do not display the same widespread connectivity areas that characterize the strong and moderate La Niña events.

The study also detected a change in the dynamics of the network structure, that coincides with the 76/77 climate shift. The networks after the climate shift exhibit conditions of lower information transfer efficiency, which are more frequent and intense than those previous to the shift and can be associated to a less stable climate.

L.C. Carpi has been supported by a scholarship from The Univ. of Newcastle. P.M. Saco also acknowledges support from the Univ. of Newcastle; O.A. Rosso from CONICET, Argentina and CNPq, Brazil; and M.G. Ravetti from FAPEMIG and CNPq, Brazil. We thank J.F. Rodriguez and C. Riveros for help during manuscript preparation.

References

1. M.S. Halpert, C.F. Ropelewski, J. Climate **5**, 577 (1992)
2. M.J. McPhaden, El Niño and La Niña: Causes and Global Consequences, in *Encyclopedia of Global Environmental Change, The Earth system: physical and chemical dimensions of global environmental change*, edited by M.C. MacCracken, J.S. Perry (Wiley, 2003), Vol. 1, pp. 353–370
3. S. Boccaletti, V. Latora, Y. Moreno, M. Chavez, D. Hwang, Phys. Rep. **424**, 175 (2006)
4. A.A. Tsonis, K.L. Swanson, G. Wang, J. Climate **21**, 2990 (2008)
5. K. Yamasaki, A. Gozolchiani, S. Havlin, Prog. Theor. Phys. Suppl. **179**, 178 (2009)
6. A.A. Tsonis, K.L. Swanson, P.J. Roebber, Bull. Am. Meteorol. Soc. **87**, 585 (2006)
7. J.F. Donges, Y. Zou, N. Marwan, J. Kurths, Eur. Phys. J. Special Top. **174**, 157 (2009)
8. A.A. Tsonis, P.J. Roebber, Phys. A **333**, 497 (2004)
9. A. Tsonis, G. Wang, K. Swanson, F. Rodrigues, L. Costa, Clim. Dyn. **37**, 933 (2011)
10. J.F. Donges, Y. Zou, N. Marwan, J. Kurths, Europhys. Lett. **87**, 48007 (2009)
11. J.F. Donges, H.C.H. Schultz, N. Marwan, Y. Zou, J. Kurths, Eur. Phys. J. B: Condens. Matter Complex Syst. **84**, 635 (2011)
12. K. Yamasaki, A. Gozolchiani, S. Havlin, Phys. Rev. Lett. **100**, 228501 (2008)
13. K. Steinhaeuser, A.R. Ganguly, N.V. Chawla, Clim. Dyn. 1 (2011), in press
14. M. Barreiro, A. Marti, C. Masoller, Chaos **21**, 013101 (2011)
15. N. Malik, B. Bookhagen, N. Marwan, J. Kurths, Clim. Dyn. 1 (2012), in press
16. A. Gozolchiani, K. Yamasaki, O. Gazit, S. Havlin, Europhys. Lett. **83**, 28005 (2008)
17. L.C. Carpi, O.A. Rosso, P.M. Saco, M.G. Ravetti, Phys. Lett. A **375**, 801 (2011)
18. A.S. Taschetto, M.H. England, J. Climate **22**, 3167 (2009)
19. A.A. Tsonis, K.L. Swanson, Phys. Rev. Lett. **100**, 228502 (2008)
20. E. Kalnay et al., Bull. Amer. Meteorol. Soc. **77**, 437 (1996)
21. K. Steinhaeuser, N.V. Chawla, A.R. Ganguly, An Exploration of Climate Data Using Complex Networks, in *Proceedings of the Third International Workshop on Knowledge Discovery from Sensor Data* (ACM, New York, NY, USA, 2009), SensorKDD '09, pp. 23–31
22. V. Latora, M. Marchiori, Phys. Rev. Lett. **87**, 198701 (2001)
23. F. Österreicher, I. Vajda, Ann. Inst. Statist. Math. **55**, 639 (2003)
24. D.M. Endres, J.E. Schindelin, IEEE Trans. Inf. Theory **49**, 1858 (2003)
25. T.M. Smith, R.W. Reynolds, T.C. Peterson, J. Lawrimore, J. Climate **21**, 2283 (2008)
26. H.L. Ren, F.F. Jin, Geophys. Res. Lett. **38**, L04704 (2011)
27. T. Lee, M.J. McPhaden, Geophys. Res. Lett. **37**, L14603 (2010)
28. S.A. Hill, D. Braha, Phys. Rev. E **82**, 046105 (2010)
29. E. Hackert, J. Ballabrera-Poy, A.J. Busalacchi, R.H. Zhang, R. Murtugudde, J. Geophys. Res. **112**, C01005 (2007)
30. M.J. McPhaden, Adv. Geosci. **14**, 219 (2008)